Article

Mispair-Aligned NT-alkyl-NT Interstrand Cross-Linked DNA: Synthesis and Characterization of Duplexes with Interstrand Cross-Links of Variable Lengths

Christopher J. Wilds, Anne M. Noronha, Sebastien Robidoux, and Paul S. Miller

J. Am. Chem. Soc., **2004**, 126 (30), 9257-9265• DOI: 10.1021/ja0498540 • Publication Date (Web): 10 July 2004

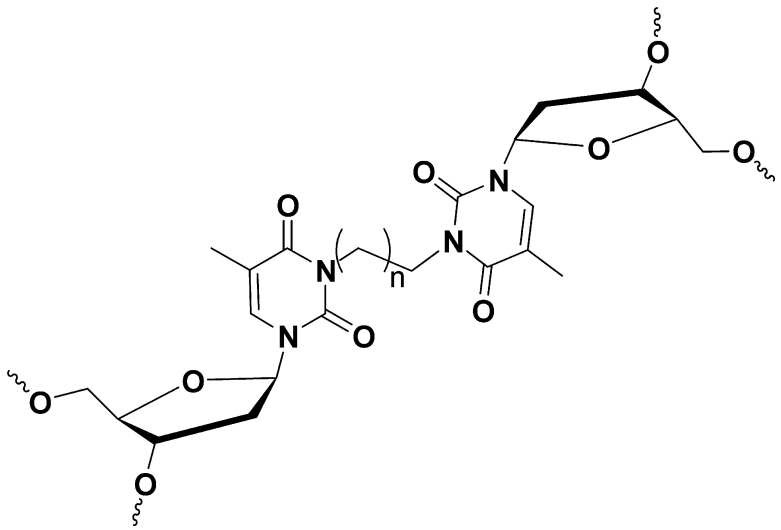

More About This Article

Additional resources and features associated with this article are available within the HTML version:

- Supporting Information
- Links to the 5 articles that cite this article, as of the time of this article download
- Access to high resolution figures
- Links to articles and content related to this article
- Copyright permission to reproduce figures and/or text from this article

View the Full Text HTML

J|A|C|S
ARTICLES
Published on Web 07/10/2004

Mispair-Aligned N^{3}T-alkyl-N^{3}T Interstrand Cross-Linked DNA: Synthesis and Characterization of Duplexes with Interstrand Cross-Links of Variable Lengths

Christopher J. Wilds,[†,‡] Anne M. Noronha,[†,§] Sebastien Robidoux,[||] and Paul S. Miller*[,†]

Contribution from the Department of Biochemistry and Molecular Biology, Bloomberg School of Public Health, Johns Hopkins University, Baltimore, Maryland, 21205, and Department of Chemistry and Biochemistry, Concordia University, Montreal, Quebec, H4B 1R6, Canada

Received January 9, 2004; E-mail: pmiller@jhsph.edu

Abstract: Therapeutic bifunctional alkylating agents generate interstrand cross-links in duplex DNA. As part of our continuing studies on DNA duplexes that contain alkyl interstrand cross-links, we have synthesized a cross-link that bridges the N^3 positions of a mismatched thymidine base pair. This cross-link, which is similar to the N^{3}C-alkyl-N^{3}C cross-link that has been observed between mismatched cytosine base pairs, was introduced by first incorporating a cross-linked phosphoramidite unit at the 5′-end of an oligonucleotide chain. Fully cross-linked duplexes were then synthesized using an orthogonal approach to selectively remove protecting groups, thus allowing construction of the cross-linked duplex via conventional solid-phase oligonucleotide synthesis. Short DNA duplexes with alkyl cross-links of various lengths (two, four, and seven methylene units) were prepared, and their physical properties were studied via UV thermal denaturation and circular dichroism spectroscopy. These linkers were found to stabilize the duplexes by 37, 31, and 16 °C for the two-, four-, and seven-carbon linkers, respectively, relative to a non-cross-linked duplex. Circular dichroism spectra suggested that these lesions induce very little deviation in the global structure relative to the non-cross-linked duplex DNA control. Molecular models show that the two-carbon cross-link spans the distance between the N^3 atoms of the T−T mismatch without perturbing the helix structure, whereas the longer linkers, particularly the seven-carbon linker, tend to push the thymines apart, creating a local distortion. This perturbation may account for the lower thermal stability of the seven-carbon versus two-carbon cross-linked duplex.

Introduction

Covalent DNA lesions play important roles in the etiology and treatment of cancer. Therapeutic alkylating agents include monofunctional and bifunctional agents. The latter category includes platinum agents, nitrogen mustards, chloroethylnitrosoureas, and cyclophosphamide.[1−4] The major cytotoxic lesion introduced by the latter three agents are interstrand cross-links, which if left unrepaired, prevent DNA strand separation and normal mitosis, interfere with transcription, and induce apoptosis.

A problem presented in cancer treatment is the development of resistance to the effects of antitumor agents, which is often due to enhanced repair of interstrand cross-links.[5−7] Although a number of repair pathways, including homologous recombination and nucleotide excision repair, have been implicated in cross-link repair in bacteria and mammalian cells, an understanding of the molecular mechanisms that are involved is still lacking.[8−10] Since development of resistance is one of the primary reasons for treatment failure, a better understanding of the processes by which interstrand cross-links are recognized and repaired could lead to the development of more effective bifunctional alkylating agents and/or treatment protocols.

To carry out biological and structural investigations, it is necessary to have access to duplexes that contain interstrand cross-links of well-defined structure. There are two general strategies employed in producing such duplexes. The first

[†] Department of Biochemistry and Molecular Biology, Johns Hopkins University.
[‡] Current address: Department of Chemistry and Biochemistry, Concordia University.
[§] Current address: Alnylam Pharmaceuticals, Cambridge, MA.
[||] Department of Chemistry and Biochemistry, Concordia University.

(1) Colvin, M. *The Alkylating Agents*; W. B. Saunders Co.: Philadelphia, 1982.
(2) Colvin, M. *Alkylating Agents and Platinum Antitumor Compounds*; Lea & Febiger: Philadelphia and London, 1993.
(3) Pratt, W. B.; Ruddon, R. W.; Ensminger, W. D.; Maybaum, J. *Covalent DNA Binding Drugs*; Oxford Press: New York, 1994.
(4) Rajski, S. R.; Williams, R. M. *Chem. Rev.* **1998**, *98*, 2723−2725.
(5) O'Connor, P. M.; Kohn, K. W. *Cancer Commun.* **1990**, *2*, 387−394.
(6) (a) Friedman, H. S.; Colvin, O. M.; Kaufmann, S. H.; Ludeman, S. M.; Bullock, N.; Bigner, D. D.; Griffith, O. W. *Cancer Res.* **1992**, *52*, 5373−5378. (b) Dong, Q.; Bullock, N.; Aliosman, F.; Colvin, O. M.; Bigner, D. D.; Friedman, H. S. *Cancer Chemother. Pharmacol.* **1996**, *37*, 242−246. (c) Dong, Q.; Johnson, S. P.; Colvin, O. M.; Bullock, N.; Kilborn, C.; Runyon, G.; Sullivan, D. M.; Easton, J.; Bigner, D. D.; Nahta, R.; Marks, J.; Modrich, P.; Friedman, H. S. *Cancer Chemother. Pharmacol.* **1999**, *43*, 73−79.
(7) Ali-Osman, F.; Raikar, A.; Young, P. *Cancer Biochem. Biophys.* **1995**, *14*, 231−241.
(8) Friedberg, E. C.; Walker, G. C.; Siede, W. *DNA Repair and Mutagenesis*; ASM Press: Washington, DC, 1995.
(9) Dronkert, M. L. G.; Kanaar, R. *Mutat. Res.* **2001**, *486*, 217−247.
(10) McHugh, P.; Spanswick, V.; Hartley, J. *Lancet Oncol.* **2001**, *2*, 483−490.

approach involves treatment of duplex DNA with an excess of bifunctional alkylating agent to produce the interstrand cross-link.[11−16] This methodology suffers from poor yields because of the production of numerous monoalkylated and other side products that must be separated from the desired cross-linked product and the low efficiency of the cross-linking reaction itself. The second and more attractive approach involves de novo synthesis of a cross-linked duplex employing a solid-phase synthesis approach.[17]

We recently described the syntheses and characterization of short DNA duplexes that contain a N^4C-ethyl-N^4C interstrand cross-link using either a phosphoramidite reagent to introduce the cross-link during automated synthesis of the cross-linked duplex or a convertible nucleoside approach.[18−21] This methodology has allowed the solid-phase syntheses of a number of novel cross-linked duplexes of well-defined structure that have been engineered to contain an interstrand cross-link between a mismatched C−C base pair,[18] a "staggered" interstrand cross-link at a −CG− or −GC− step,[20] as well as 1,3 interstrand −CNG− cross-links containing alkyl linkages of various lengths.[21] The latter are of particular interest because they share similarities to the interstrand cross-links formed by reaction of duplex DNA with bifunctional alkylators, such as mechlorethamine, which forms a N^7G-alkyl-N^7G cross-link in sequences containing a −GNC− sequence motif.

As part of our investigation of interstrand cross-linked DNA, we have developed a straightforward synthesis of a novel interstrand N^3T-alkyl-N^3T cross-link. This lesion is similar to the recently discovered N^3C-alkyl-N^3C cross-link formed when duplex DNA containing a C−C mismatch is treated with mechlorethamine.[22,23] In this report, we describe the syntheses of short DNA duplexes that contain N^3T-alkyl-N^3T interstrand cross-links and preliminary characterization of their physical properties.

Experimental Section

Materials and General Methods. 5′-*O*-Dimethoxytrityl-2′-deoxythymidine was purchased from ChemGenes Inc., Ashland, MA. 5′-*O*-Dimethoxytrityl-3′-*O*-*tert*-butyldimethylsilyl-2′-deoxythymidine (**1**) was prepared as previously described.[18] 5′-*O*-Dimethoxytrityldeoxyribonucleoside-3′-*O*-(*β*-cyanoethyl-*N*,*N*′-diisopropyl) phosphoramidites, 3′-*O*-dimethoxytrityldeoxyribonucleoside-5′-*O*-(*β*-cyanoethyl-*N*,*N*′-diisopropyl)-phosphoramidites, and protected deoxyribonucleoside-controlled pore glass supports were purchased from Glen Research, Inc. (Sterling, VA) and ChemGenes, respectively. All other chemicals and solvents were purchased from Aldrich Chemical Co. (Milwaukee, WI). 2-Iodoethyl phenoxyacetate was prepared from 2-iodoethanol and phenoxyacetyl chloride. Both 4-iodobutyl phenoxyacetate and 7-iodoheptylphenoxyacetate were prepared by a two-step reaction: the corresponding 1,4- and 1,7-diols (50 equiv) were reacted with phenoxyacetyl chloride (1 equiv), followed by the conversion of the free alcohol to an iodide.[24] Strong anion exchange (SAX) HPLC was carried out using a Dionex DNAPAC PA-100 column (0.4 cm × 25 cm) purchased from Dionex Corp, Sunnyvale, CA. Reversed-phase HPLC was carried out using a Microsorb-C-18 column (0.46 × 15 cm) purchased from Varian Associates, Walnut Creek, CA. The SAX column was eluted with a 30 mL linear gradient of sodium chloride in a buffer that contained 100 mM Tris (pH 7.8) in 10% acetonitrile at a flow rate of 1.0 mL/min. The C-18 column was eluted with a 20 mL linear gradient of acetonitrile in 50 mM phosphate buffer (pH 5.8) at a flow rate of 1.0 mL/min. The columns were monitored at 260 nm for analytical runs or 290 nm for preparative runs. Denaturing polyacrylamide gel electrophoresis was carried out on 20 cm × 20 cm × 0.75 cm gels containing 20% acrylamide and 7 M urea in TBE, which contained 89 mM Tris, 89 mM boric acid, and 0.2 mM ethylenediaminetetraacetate buffered at pH 8.0. The running buffer was TBE. [^{32}P]-Labeled oligonucleotides were detected by autoradiography. Mass spectra were obtained at the John Hopkins University School of Medicine Mass Spectrometry Facility (MALDI) or from the Scripps Research Institute Mass Spectrometry Facility (ESI).

5′-*O*-Dimethoxytrityl-3′-*O*-phenoxyacetyl-2′-deoxythymidine, 2.[25] 5′-*O*-Dimethoxytrityl-2′-deoxythymidine (4.0 g, 7.36 mmol) was dissolved in THF (20 mL) and allowed to cool to 0 °C. Triethylamine (1.19 g, 11.72 mmol) followed by phenoxyacetyl chloride (1.89 g, 11.0 mmol) was added dropwise. After 14 h, the solvent was removed in vacuo, the crude product was taken up in dichloromethane (50 mL), and the solution was washed with three portions of sodium bicarbonate (3 × 50 mL). The organic layer was dried over sodium sulfate and concentrated to give a yellow gum. The crude product was purified by column chromatography using dichloromethane/methanol (49:1) to afford 3.95 g (79.3%) of product as a colorless foam. R_f (SiO_2 TLC): 0.31 dichloromethane/methanol (19:1).^{1}H NMR (400 MHz, DMSO-d_6, ppm): 1.41 (3H, C5−CH_3), 2.32−2.52 (2H, H2′ and H2″), 3.18−3.34 (2 H, H5′ and H5″), 3.71 (6H, −OCH_3), 4.10−4.11 (1H, H4′), 4.80 (2 H, −CH_2OPh), 5.38−5.40 (1H, H3′), 6.19−6.23 (1 H, H1′), 6.84−7.38 (18 H, DMT, Ph), 7.51 (1 H, H6). ESI-MS (M + Na^+): 701 (calcd 701).

N^3-[2-(Phenoxyacetyl)ethyl]-5′-*O*-dimethoxytrityl-3′-*O*-(*tert*-butyldimethylsilyl)-2′-deoxythymidine, 3a. 5′-*O*-Dimethoxytrityl-3′-*O*-(*tert*-butyldimethylsilyl)-2′-deoxythymidine **1** (5.0 g, 7.59 mmol) was dissolved in acetonitrile (200 mL). Then, 2-iodoethyl phenoxyacetate (4.7 g, 15.35 mmol) was added, followed by the addition of 1,8-diazabicyclo[5.4.0]undec-7-ene (2.36 g, 15.51 mmol). After 24 h, the solvent was removed in vacuo, the crude product was taken up in dichloromethane (200 mL), and the solution was washed with three portions of sodium bicarbonate (3 × 200 mL). The organic layer was dried over sodium sulfate, and the crude compound was purified by silica gel column chromatography using hexanes/ethyl acetate (4:1) to afford 5.51 g (87.5%) of the product as a colorless foam. R_f (SiO_2 TLC): 0.66 hexanes/ethyl acetate (1:1). ^{1}H NMR (400 MHz): 0.00 (3H, $SiCH_3$), 0.05 (3H, $SiCH_3$), 0.83 (9H, Si−C(CH_3)$_3$), 1.61 (3H, C5−CH_3), 2.20−2.41 (2H, H2′ and H2″), 3.22−3.38 (2 H, H5′ and H5″), 3.79 (6H, −OCH_3), 3.81−3.92 (1H, H4′), 4.15−4.18 (2H, CH_2−N^3), 4.37−4.41 (2H, CH_2−OPac), 4.49−4.53 (1H, H3′), 4.72 (2 H, −CH_2OPh), 6.24−6.27 (1 H, H1′), 6.94−7.46 (18 H, DMT, Ph), 7.70 (1 H, H6). ESI-MS: 837 (calcd 836.4).

N^3-[4-(Phenoxyacetyl)butyl]-5′-*O*-dimethoxytrityl-3′-*O*-(*tert*-butyldimethylsilyl)-2′-deoxythymidine, 3b. Compound **3b** was synthe-

(11) Ojwang, J. O.; Grueneberg, D. A.; Loechler, E. L. *Cancer Res.* **1989**, *49*, 6529−6537.
(12) Rink, S. M.; Solomon, M. S.; Taylor, M. J.; Rajur, S. B.; McLaughlin, L. W.; Hopkins, P. B. *J. Am. Chem. Soc.* **1993**, *115*, 2551−2557.
(13) Tsarouhtsis, D.; Kuchimanchi, S.; Decorte, B. L.; Harris, C. M.; Harris, T. M. *J. Am. Chem. Soc.* **1995**, *117*, 11013−11014.
(14) Rink, S. M.; Lipman, R.; Alley, S. C.; Hopkins, P. B.; Tomasz, M. *Chem. Res. Toxicol.* **1996**, *9*, 382−389.
(15) Warren, A. J.; Hamilton, J. W. *Chem. Res. Toxicol.* **1996**, *9*, 1063−1071.
(16) Fischhaber, P. L.; Gall, A. S.; Duncan, J. A.; Hopkins, P. B. *Cancer Res.* **1999**, *59*, 4363−4368.
(17) Harwood, E. A.; Sigurdsson, S. T.; Edfeldt, N. B. F.; Reid, B. R.; Hopkins, P. B. *J. Am. Chem. Soc.* **1999**, *121*, 5081−5082.
(18) Noll, D. M.; Noronha, A. M.; Miller, P. S. *J. Am. Chem. Soc.* **2001**, *123* 3405−3411.
(19) Noronha, A. M.; Noll, D. M.; Miller, P. S. *Nucleosides Nucleotides Nucleic Acids* **2001**, *20*, 1303−1307.
(20) Noronha, A. M.; Noll, D. M.; Wilds, C. J.; Miller, P. S. *Biochemistry* **2002**, *41*, 760−771.
(21) Noronha, A. M.; Wilds, C. J.; Miller, P. S. *Biochemistry* **2002**, *41*, 8605−8612.
(22) Romero, R. M.; Rojsitthisak, P.; Haworth, I. S. *Arch. Biochem. Biophys.* **2001**, *386*, 143−153.
(23) Romero, R. M.; Mitas, M.; Haworth, I. S. *Biochemistry* **1999**, *38*, 3641−3648.
(24) Garegg, P. J.; Samuelsson, B. J. C. S. *Chem. Commun.* **1979**, 978−980.
(25) Nikiforov, T.; Connolly, B. A. *Tetrahedron Lett.* **1992**, *33*, 2379−2382.

sized via the procedure outlined for **3a** using 4-iodobutyl phenoxyacetate to afford the desired product in 82.2% yield. R_f (SiO_2 TLC): 0.69 hexanes/ethyl acetate (1:1). ^{1}H NMR (400 MHz, DMSO-d_6, ppm): 0.00 (3H, Si−CH_3), 0.06 (3H, Si−CH_3), 0.83 (9 H, Si−$C(CH_3)_3$), 1.52−1.70 (7H, −CH_2−CH_2− and C5−CH_3), 2.19−2.41 (2 H, H2′ and H2″), 3.20−3.33 (2 H, H5′ and H5″), 3.78 (6H, −OCH_3), 3.82−3.86 (2H, −CH_2−N^3−), 3.87−3.90 (1H, H4′), 4.15−4.18 (2H, −CH_2−OPac), 4.50−4.54 (1H, H3′), 4.82 (2H, OCH_2OPh), 6.26 (1H, H1′), 6.92−7.67 (18 H, DMT, Ph), 7.67 (H6). ESI-MS (M + H^+): 866 (calcd 865.09).

N³-[7-(Phenoxyacetyl)heptyl]-5′-*O*-dimethoxytrityl-3′-*O*-(*tert*-butyldimethylsilyl)-2′-deoxythymidine, 3c. Compound **3c** was synthesized via the procedure outlined for **3a** using 7-iodoheptyl phenoxyacetate to afford the desired product in 80.0% yield. R_f (SiO_2 TLC): 0.52 hexanes/ethyl acetate (1:1)

^{1}H NMR (400 MHz, DMSO-d_6, ppm): 0.00 (3H, Si−CH_3), 0.06 (3H, Si−CH_3), 0.83 (9 H, Si−$C(CH_3)_3$), 1.29 (4H, −CH_2−CH_2−), 1.52−1.62 (9H, −CH_2−CH_2− and C5−CH_3), 2.20−2.41 (2 H, H2′ and H2″), 3.21−3.35 (2 H, H5′ and H5″), 3.77 (6H, −OCH_3), 3.81−3.85 (2H, −CH_2−N^3−), 3.88−3.91 (1H, H4′), 4.13−4.16 (2H, −CH_2−OPac), 4.51−4.55 (1H, H3′), 4.82 (2H, OCH_2OPh), 6.25−6.28 (1H, H1′), 6.92−7.46 (18 H, DMT, Ph), 7.67 (H6). ESI-MS (M + H^+): 907 (calcd 906.4).

N³-(2-Iodoethyl-)-5′-*O*-dimethoxytrityl-3′-*O*-(*tert*-butyldimethylsilyl)-2′-deoxythymidine, 4a. Compound **3a** (5.51 g, 6.58 mmol) was dissolved in dichloromethane (50 mL), and propylamine (15 mL) was added dropwise to the solution. After 24 h, the solvent was removed in vacuo, the crude product was taken up in dichloromethane (250 mL), and the solution was washed with three portions of sodium bicarbonate (3 × 200 mL). The organic layer was dried over sodium sulfate and evaporated to afford the crude 2-hydroxyethyl intermediate, which was dissolved in THF (200 mL) and cooled to 0 °C. Imidazole (2.95 g, 43.47 mmol), triphenylphosphine (5.70 g, 21.74 mmol), and iodine (5.51 g, 21.74 mmol) were added sequentially. After 3 h, the solvent was removed in vacuo, the crude product was taken up in dichloromethane (200 mL), and the solution was washed with sodium thiosulfate (10%, 3 × 100 mL), dried over sodium sulfate, and then evaporated. The crude product was purified via silica gel column chromatography using hexanes/ethyl acetate (4:1) as eluent to afford 4.42 g (82.1%) of the desired compound as a colorless foam. R_f (SiO_2 TLC): 0.85 hexanes/ethyl acetate (1:1). ^{1}H NMR (400 MHz): 0.00 (3H, $SiCH_3$), 0.06 (3H, $SiCH_3$), 0.83 (9H, Si−$C(CH_3)_3$), 1.60 (3H, C5−CH_3), 2.19−2.42 (2H, H2′ and H2″), 3.20−3.34 (4 H, CH_2−I, H5′ and H5″), 3.79 (6H, −OCH_3), 3.88−3.90 (1H, H4′), 4.16−4.20 (2H, CH_2−N^3), 4.49−4.54 (1H, H3′), 6.22−6.25 (1 H, H1′), 6.93−7.45 (14 H, DMT), 7.69 (1 H, H6). ESI-MS (M + H^+): 813 (calcd 812.2).

N³-(2-Iodobutyl-)-5′-*O*-dimethoxytrityl-3′-*O*-(*tert*-butyldimethylsilyl)-2′-deoxythymidine, 4b. Compound **4b** was synthesized via the procedure outlined for **4a** to afford the desired product in 85.8% yield. R_f (SiO_2 TLC): 0.74 hexanes/ethyl acetate (1:1). ^{1}H NMR (400 MHz, DMSO-d_6, ppm): −0.05 (3H, Si−CH_3), 0.01 (3H, Si−CH_3), 0.78 (9 H, Si−$C(CH_3)_3$), 1.55 (3H, C5−CH_3), 1.57−1.78 (4H, −CH_2−CH_2−), 2.14−2.36 (2 H, H2′ and H2″), 3.14−3.31 (4 H, −CH_2−I−, H5′ and H5″), 3.73 (6H, −OCH_3), 3.80−3.84 (3H, −CH_2−N^3−, H4′), 4.45−4.49 (1H, H3′), 6.18−6.21 (1H, H1′), 6.87−7.40 (13 H, DMT), 7.61 (H6). ESI-MS (M + H^+): 841 (calcd 840.9).

N³-(2-Iodoheptyl)-5′-*O*-dimethoxytrityl-3′-*O*-(*tert*-butyl-dimethylsilyl)-2′-deoxythymidine, 4c. Compound **4c** was synthesized via the procedure outlined for **4a** to afford the desired product in 75.2% yield. R_f (SiO_2 TLC): 0.67 hexanes/ethyl acetate (1:1). ^{1}H NMR (400 MHz): (400 MHz, DMSO-d_6, ppm): 0.00 (3H, Si−CH_3), 0.06 (3H, Si−CH_3), 0.83 (9 H, Si−$C(CH_3)_3$), 1.28−1.39 (6H, −CH_2−CH_2−CH_2−), 1.52−1.56 (2H, −CH_2−), 1.60 (3H, C5−CH_3), 1.74−1.80 (2H, −CH_2−), 2.19−2.41 (2 H, H2′ and H2″), 3.19−3.33 (4 H, −CH_2−I−, H5′ and H5″), 3.78 (6H, −OCH_3), 3.81−3.85 (2H, −CH_2−N^3−), 3.86−3.89 (1H, H4′), 4.49−4.53 (1H, H3′), 6.23−6.26 (1H, H1′), 6.92−7.45 (13 H, DMT), 7.65 (1H, H6). ESI-MS (M + H^+): 883 (calcd 882.3).

1-{N³-[5′-*O*-(Dimethoxytrityl)-3′-*O*-(*tert*-butyldimethylsilyl)-2′-deoxythymidylyl]}-2-{N³-[5′-*O*-(dimethoxytrityl)-3′-*O*-(phenoxyacetyl)-2′-deoxythymidylyl]}ethane, 5a. Compound **2** (3.68 g, 5.44 mmol) was dissolved in acetonitrile (100 mL). Compound **4a** (4.42 g, 5.44 mmol) was added, followed by the addition of 1,8-diazabicyclo[5.4.0]-undec-7-ene (0.83 g, 5.44 mmol). After 24 h, the solvent was removed in vacuo, the product was taken up in dichloromethane (100 mL), and the solution was washed with three portions of sodium bicarbonate (3 × 100 mL). The organic layer was dried over sodium sulfate, and the crude product was purified by silica gel column chromatography using hexanes/ethyl acetate (2:3) to afford 5.82 g (78.5%) of the product as a colorless foam. R_f (SiO_2 TLC): 0.44 hexanes/ethyl acetate (1:1).

^{1}H NMR (400 MHz): 0.00 (3H, Si−CH_3), 0.05 (3H, Si−CH_3), 0.84 (9H, Si−$C(CH_3)_3$), 1.49 (3H, C5−CH_3), 1.56 (3H, C5−CH_3), 2.16−2.56 (4H, H2′ and H2″), 3.23−3.42 (4H, H5′ and H5″), 3.44 (12 H, −OCH_3), 3.90−3.91 (1H, H4′), 4.09−4.24 (5H, H4′ and − N^3−CH_2−CH_2−N^3−), 4.49−4.53 (1H, H3′), 4.83 (2H, −CH_2OPh), 5.48−5.50 (1H, H3′), 6.18−6.32 (2H, H1′), 6.95−7.48 (52H, DMT, Ph), 7.60 (1H, H6), 7.64 (1H, H6). ESI-MS (M + Na^+): 1386 (calcd 1386).

1-{N³-[5′-*O*-(Dimethoxytrityl)-3′-*O*-(*tert*-butyldimethylsilyl)-2′-deoxythymidylyl]}-4-{N³-[5′-*O*-(dimethoxytrityl)-3′-*O*-(phenoxyacetyl)-2′-deoxythymidylyl]}butane, 5b. Compound **5b** was synthesized via the procedure outlined for **5a** to afford the desired product in 69.6% yield. R_f (SiO_2 TLC): 0.47 hexanes/ethyl acetate (1:1). ^{1}H NMR (400 MHz, DMSO-d_6, ppm): 0.00 (3H, Si−CH_3), 0.06 (3H, Si−CH_3), 0.83 (9 H, Si−$C(CH_3)_3$), 1.50−1.56 (7H, C5−CH_3, −CH_2−CH_2−), 1.59 (3 H, C5−CH_3), 2.20−2.48 (4 H, H2′ and H2″), 3.19−3.35 (4 H, H5′ and H5″), 3.78 (12H, −OCH_3), 3.80−3.90 (5H, H4′, −CH_2−N^3), 4.19−4.22 (1H, H4′), 4.49−4.53 (1H, H3′), 4.87 (2H, OCH_2OPh), 5.46−5.49 (1H, H3′), 6.23−6.34 (2H, H1′), 6.92−7.45 (31 H, DMT, Ph), 7.64−7.66 (2H, H6). ESI-MS (M + H^+): 1392 (calcd 1391.7).

1-{N³-[5′-*O*-(Dimethoxytrityl)-3′-*O*-(*tert*-butyldimethylsilyl)-2′-deoxythymidylyl]}-7-{N³-[5′-*O*-(dimethoxytrityl)-3′-*O*-(phenoxyacetyl)-2′-deoxythymidylyl]}heptane, 5c. Compound **5c** was synthesized via the procedure outlined for **5a** to afford the desired product in 98.2% yield. R_f (SiO_2 TLC): 0.45 hexanes/ethyl acetate (1:1). ^{1}H NMR (400 MHz, DMSO-d_6, ppm): 0.00 (3H, Si−CH_3), 0.06 (3H, Si−CH_3), 0.83 (9 H, Si−$C(CH_3)_3$), 1.12−1.17 (4H, −CH_2−CH_2−), 1.54 (3H, C5−CH_3), 1.60 (3 H, C5−CH_3), 2.21−2.48 (4 H, H2′ and H2″), 3.19−3.35 (4 H, H5′ and H5″), 3.37−3.46 (4H, −CH_2−N^3), 3.78 (12H, −OCH_3), 3.87−3.90 (1H, H4′), 4.49−4.53 (3H, H3′), 4.87 (2H, OCH_2OPh), 6.23−6.34 (2H, H1′), 6.92−7.45 (31 H, DMT, Ph), 7.63−7.66 (2H, H6). ESI-MS (M + H^+): 1434 (calcd 1432.7).

1-{N³-[5′-*O*-(Dimethoxytrityl)-3′-*O*-(*tert*-butyldimethylsilyl)-2′-deoxythymidylyl]}-2-{N³-[5′-*O*-(dimethoxytrityl)-2′-deoxythymidylyl]}-ethane, 6a. Compound **5b** (5.38 g, 3.95 mmol) was dissolved in dichloromethane (50 mL), and propylamine (10 mL) was added. After 12 h, the solvent was removed in vacuo, the crude product was taken up in dichloromethane (100 mL), and the solution was washed with three portions of sodium bicarbonate (3 × 100 mL). The organic layer was dried over sodium sulfate and evaporated to afford the crude product, which was purified via silica gel column chromatography using hexanes/ethyl acetate (2:3) as eluent to afford 4.64 g (82.1%) of the desired compound as a colorless foam. R_f (SiO_2 TLC): 0.15 hexanes/ethyl acetate (1:1). ^{1}H NMR (400 MHz, DMSO-d_6, ppm): 0.00 (3H, Si−CH_3), 0.05 (3H, Si−CH_3), 0.83 (9H, Si−$C(CH_3)_3$), 1.49 (3H, C5−CH_3), 1.54 (3H, C5−CH_3), 2.18−2.37 (4H, H2′ and H2″), 3.23−3.40 (4H, H5′ and H5″), 3.44 (12 H, −OCH_3), 3.88−3.92 (1H, H4′), 3.96−4.00 (1H, H4′), 4.49−4.53 (1H, H3′), 4.12−4.24 (4H, −N^3−CH_2−CH_2−N^3−), 4.35−4.39 (1H, H3′), 4.49−4.54 (1H, H3′), 6.17−6.26 (2H, H1′), 6.95−7.48 (26 H, DMT), 7.58 (1H, H6), 7.64 (1H, H6). ESI-MS (M + H^+): 1229.5 (calcd 1228.5).

1-{N³-[5′-*O*-(Dimethoxytrityl)-3′-*O*-(*tert*-butyldimethylsilyl)-2′-deoxythymidylyl]}-4-{N³-[5′-*O*-(dimethoxytrityl)-2′-deoxythymidylyl]}-butane, 6b. Compound **6b** was synthesized via the procedure outlined for **6a** to afford the desired product in 98.1% yield. R_f (SiO_2 TLC): 0.13 hexanes/ethyl acetate (1:1). ^{1}H NMR (400 MHz, DMSO-d_6, ppm): 0.00 (3H, Si−CH_3), 0.06 (3H, Si−CH_3), 0.832 (9 H, Si−C(CH_3)$_3$), 1.48−1.53 (7H, −CH_2−CH_2− and C5−CH_3), 1.59 (3H, C5−CH_3), 2.19−2.41 (4 H, H2′ and H2″), 3.20−3.34 (4H, H5′ and H5″), 3.78 (12H, −OCH_3), 3.80−3.97 (6H, H4′, −CH_2−N^3−), 4.37−4.40 (1H, H3′), 4.49−4.53 (1H, H3′), 6.23−6.31 (2H, H1′), 6 .93−7.45 (26 H, DMT), 7.62 (H6), 7.67 (H6). ESI-MS (M + Na^+): 1280 (calcd 1280).

1-{N³-[5′-*O*-(Dimethoxytrityl)-3′-*O*-(*tert*-butyldimethylsilyl)-2′-deoxythymidylyl]}-7-{N³-[5′-*O*-(dimethoxytrityl)-2′-deoxythymidylyl]}-heptane, 6c. Compound **6c** was synthesized via the procedure outlined for **6a** to afford the desired product in 94.2% yield. R_f (SiO_2 TLC): 0.28 hexanes/ethyl acetate (1:1). ^{1}H NMR (400 MHz, DMSO-d_6, ppm): 0.00 (3H, Si−CH_3), 0.06 (3H, Si−CH_3), 0.83 (9 H, Si−C(CH_3)$_3$), 1.12−1.17 (4H, −CH_2−CH_2−), 1.54 (3H, C5−CH_3), 1.60 (3 H, C5−CH_3), 2.21−2.48 (4 H, H2′ and H2″), 3.19−3.35 (4 H, H5′ and H5″), 3.37−3.46 (4H, −CH_2−N^3), 3.78 (12H, −OCH_3), 3.87−3.90 (1H, H4′), 4.49−4.53 (3H, H3′), 6.23−6.34 (2H, H1′), 6.92−7.45 (26 H, DMT, Ph), 7.63−7.66 (2H, H6). ESI-MS (M + H^+): 1300 (calcd 1298.6).

1-{N³-[5′-*O*-(Dimethoxytrityl)-3′-*O*-(*tert*-butyldimethylsilyl)-2′-deoxythymidylyl]}-2-{N³-[5′-*O*-(dimethoxytrityl)-2′-deoxythymidyl-3′-*O*-(*β*-cyanoethyl *N,N*′-diisopropyl)phosphoramidite]}ethane, 7a. Compound **6a** (0.500 g, 0.407 mmol) was dissolved in dichloromethane (2.5 mL) and diisopropylamine tetrazolide (0.243 g 1.42 mmol) added. *N,N,N*′,*N*′-2-cyanotetraisopropylphosphorane (0.441 g, 1.46 mmol) was added. After 4 h, the reaction was quenched by the addition of dichloromethane (50 mL), and the solution was extracted with sodium bicarbonate (5%, 3 × 50 mL). The organic layer was dried over sodium sulfate and evaporated to afford the crude product, which was precipitated from hexanes to yield 0.41 g (70.6%) of product as a colorless powder. R_f (SiO_2 TLC): 0.47 hexanes/ethyl acetate (1:1). ^{31}P NMR (161.8 MHz, acetone-d_6, ppm): 149.2, 149.5. ESI-MS (M + K^+): 1453 (calcd 1453.6).

1-{N³-[5′-*O*-(Dimethoxytrityl)-3′-*O*-(*tert*-butyldimethylsilyl)-2′-deoxythymidylyl]}-4-{N³-[5′-*O*-(dimethoxytrityl)-2′-deoxythymidyl-3′-*O*-(*β*-cyanoethyl *N,N*′-diisopropyl)phosphoramidite]}butane, 7b. Compound **7b** was synthesized via the procedure outlined for **7a** to afford the desired product in 85.6% yield. R_f (SiO_2): 0.50 hexanes/ethyl acetate (1:1) ^{31}P NMR (161.8 MHz, acetone-d_6, ppm): 149.2, 149.3. ESI-MS (M + K^+): 1481 (calcd 1481.6).

1-{N³-[5′-*O*-(Dimethoxytrityl)-3′-*O*-(*tert*-butyldimethylsilyl)-2′-deoxythymidylyl]}-7-{N³-[5′-*O*-(dimethoxytrityl)-2′-deoxythymidyl-3′-*O*-(*β*-cyanoethyl *N,N*′-diisopropyl)phosphoramidite]}heptane, 7c. Compound **7c** was synthesized via the procedure outlined for **7a** to afford the desired product in 72.0% yield. R_f (SiO_2 TLC): 0.52 hexanes/ethyl acetate (1:1). ^{31}P NMR (161.8 MHz, acetone-d_6, ppm): 149.0, 149.1. ESI-MS (M + H^+): 1499 (calcd 1498.8).

Syntheses and Purification of Cross-Linked Duplexes. The cross-linked duplexes, whose sequences are shown in Figure 1, were assembled on an Applied Biosystems model 392A synthesizer using standard cyanoethylphosphoramidite chemistry.[26] Long-chain alkylamine-controlled pore glass (CPG) was used as the solid support. The nucleoside phosphoramidites were prepared in anhydrous acetonitrile at a concentration of 0.15 M for the 3′-phosphoramidites or 0.3 M for the 5′-phosphoramidites. Assembly of sequences was carried out as follows: (a) detritylation: 2% dichloroacetic acid in dichloromethane; (b) nucleoside phosphoramidite coupling time of 2 min for commercial phosphoramidites and 10 min for the T−T cross-linked phosphoramidite; (c) capping: 1:1 (v/v) of acetic anhydride/collidine/tetrahydrofuran 1:1:8 (v/v/v/; solution A) and 1-methyl-1 *H*-imidazole/tetrahydrofuran 16:84 (w/v; solution B); (d) oxidation: 0.1 M iodine in tetrahydrofuran/water/pyridine 2.5:2:1. The cyanoethyl groups were removed from the CPG-linked oligomers by treating the support with 1 mL of anhydrous triethylamine (TEA) for at least 12 h. The support was washed with 30 mL of anhydrous acetonitrile followed by anhydrous tetrahydrofuran. The *tert*-butyldimethylsilyl group was removed from the partial duplex by treating the support with 1 mL of 1.0 M solution of tetra-*n*-butylammonium fluoride in tetrahydrofuran (stored over molecular sieves) for 20 min. The support was then washed with 30 mL of anhydrous tetrahydrofuran and 30 mL of acetonitrile and then dried via high vacuum (20 min). The last segment of the duplex was then synthesized using 5′ phosphoramidites with a total detritylation exposure of 130 s. The 3′-terminal trityl group was removed by the synthesizer.

The oligomer-derivatized CPG was transferred from the reaction column to autosampler vials fitted with Teflon-lined caps, and the protecting groups were removed by treatment with a mixture of concentrated ammonium hydroxide: ethanol (0.3 mL:0.1 mL) for 4 h at 55 °C. The cross-linked duplexes were purified by SAX HPLC. The retention times of the duplexes are given in Table 1. The purified oligomers were desalted using C-18 SEP PAK cartridges (Waters, Inc.). The amounts of purified oligomers obtained are shown in Table 1.

The cross-linked oligomers (0.2 A_{260} unit) were characterized by digestion with a combination of snake venom phosphodiesterase (0.28 unit) and calf intestinal phosphatase (5 units) in a buffer containing 10 mM Tris (pH 8.1) and 2 mM magnesium chloride as previously described.[18] The resulting mixture of nucleosides was analyzed by reversed-phase HPLC, and the ratio of nucleosides was determined. The results are given in Table 1. The molecular weights of each cross-

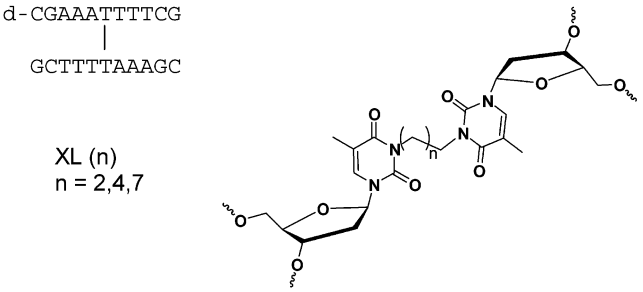

Figure 1. Sequences of the cross-linked duplexes. The 5′ end of each strand of the duplex is denoted by "d-". The structure of the N^3T-ethyl-N^3T cross-link is shown at the right.

Table 1. Amounts, Retention Times, Nucleoside Ratios, and Mass Spectral Data for Cross-Linked Duplexes

cross-linked duplexes	A_{260} units[a]	retention time[b]	nucleoside composition	Nucleoside Ratios		Mass	
				expected	observed	expected	observed
XL-2	272 (22)	26.3	dC	1.00	1.00	6687.21	6691.05
			dG	1.00	1.19		
			dT	1.50	1.81		
			dA	1.50	1.53		
			dT-dT	0.25	0.22		
XL-4	153 (24)	26.4	dC	1.00	1.0	6717.08	6718.78
			dG	1.00	1.19		
			dT	1.50	1.82		
			dA	1.50	1.51		
			dT-dT	0.25	0.22		
XL-7	168 (21)	26.7	dC	1.00	1.0	6759.03	6759.82
			dG	1.00	1.07		
			dT	1.50	1.64		
			dA	1.50	1.58		
			dT-dT	0.25	0.20		

[a] Amount of crude cross-linked duplex purified by SAX HPLC. The numbers in parentheses indicate the amount of pure duplex obtained. [b] Retention times (in minutes) of cross-linked duplexes on SAX HPLC using a 0.0−0.5 M linear gradient of sodium chloride.

(26) Beaucage, S.; Caruthers, M. H. *Tetrahedron Lett.* **1981**, *22*, 1859−1862.

Scheme 1. Synthesis of the N³T-alkyl-N³T Cross-Link[a]

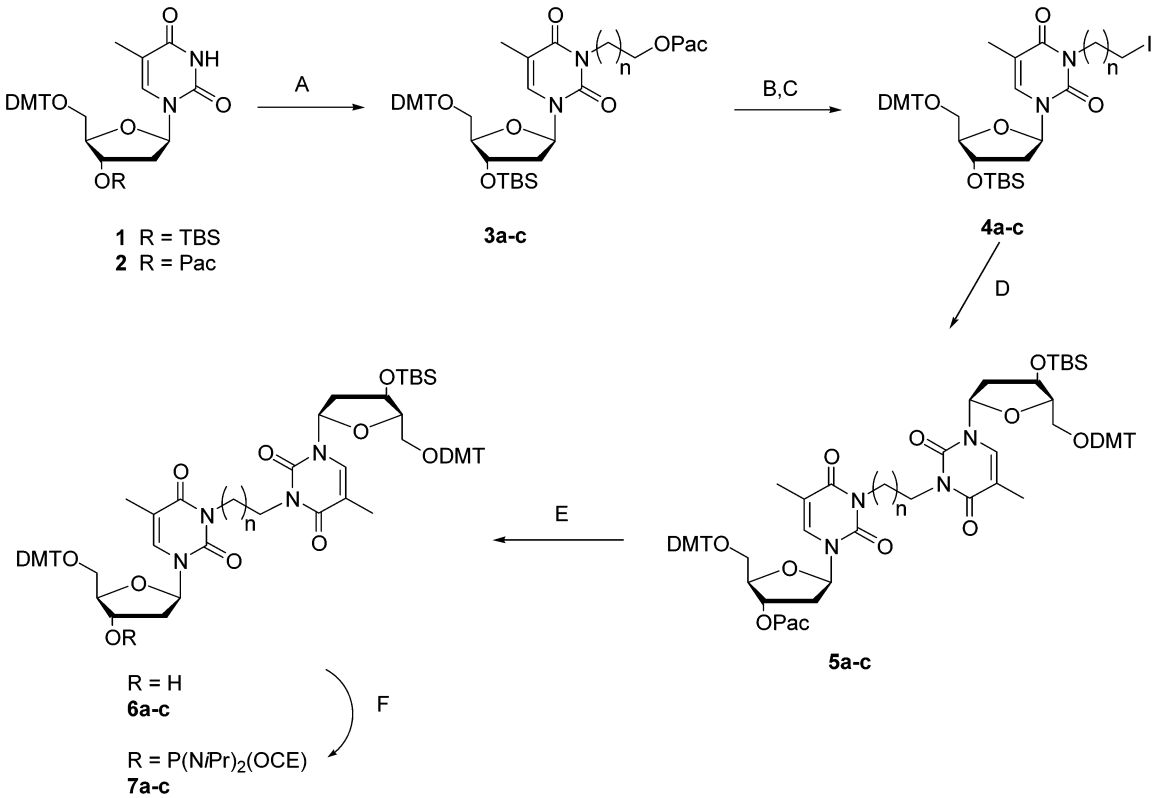

[a] (A) Compound **1**, I−CH_2−$(CH_2)_n$−OPac (where n = 1, 3, or 6; 2 equiv), DBU (2.05 equiv), acetonitrile, 24 h. (B) Propylamine/CH_2Cl_2 (4:1), 12 h. (C) Ph_3P (3.3 equiv), imidazole (6.6 equiv), I_2 (3.3 equiv), THF, 3 h. (D) Compound (**2**) (1 equiv), DBU (2 equiv), acetonitrile, 24 h. (E) Propylamine/CH_2Cl_2 (5:1), 12 h. (F) P(OCE)(N*i*Pr$_2$)$_2$ (3.6 equiv), diisopropyltetrazolide (3.5 equiv), CH_2Cl_2, 2 h.

linked oligomer were determined by MALDI-TOF mass spectrometry, and the results are shown in Table 1.

UV Thermal Denaturation Studies. Molar extinction coefficients for the oligonucleotides and cross-linked duplexes were calculated from those of the mononucleotides and dinucleotides according to nearest-neighbor approximations (units = 10^4 M^{-1} cm^{-1}).[27] Non-cross-linked duplexes were prepared by mixing equimolar amounts of the interacting strands and lyophilizing the resulting mixture to dryness. The resulting pellet was then redissolved in 90 mM sodium chloride, 10 mM sodium phosphate, and 1 mM EDTA buffer (pH 7.0) to give a final concentration of 2 μM in each strand. The cross-linked duplexes were dissolved in the same buffer to give a final concentration of 2 μM. The solutions were then heated to 65 °C for 15 min, cooled slowly to room temperature, and stored at 4 °C overnight before measurements. Prior to the thermal run, samples were degassed by placing them in a speed-vac concentrator for 2 min. Denaturation curves were acquired at 260 nm at a rate of heating of 0.5 °C/min., using a Varian CARY model 3E spectrophotometer fitted with a six-sample thermostated cell block and a temperature controller. The data were analyzed in accordance with the convention of Puglisi and Tinoco[27] and transferred to Microsoft Excel.

Circular Dichroism (CD) Spectra Spectroscopy. Circular dichroism spectra were obtained on a Jasco J-700 spectropolarimeter equipped with a NESLAB RTE-111 circulating bath. Samples were allowed to equilibrate for 5−10 min at 5 °C in 90 mM sodium chloride, 10 mM sodium phosphate, and 1 mM EDTA (pH 7.0), at a final concentration of 2 μM in each strand for the cross-linked duplexes and ca. 4 μM for control duplexes. Each spectrum is an average of 5 scans. Spectra were collected at a rate of 100 nm/min with a bandwidth of 1 nm and sampling wavelength of 0.2 nm using fused quartz cells (Hellma, 165-QS). The CD spectra were recorded from 350 to 200 nm at 5 °C. The molar ellipticity was calculated from the equation $[\theta] = \theta/Cl$, where θ is the relative ellipticity (mdeg), C is the molar concentration of oligonucleotides (mol/L), and l is the path length of the cell (cm). The data were processed on a PC computer using Windows-based software supplied by the manufacturer (JASCO, Inc.) and transferred into Microsoft Excel for presentation.

(27) Puglisi, J. D.; Tinoco, I., Jr. *Methods Enzymol*. **1989**, *180*, 304−325.

Results and Discussion

Syntheses and Characterization of Cross-Linked Duplexes. The structures of the N³T-alkyl-N³T cross-links and the cross-linked duplexes are shown in Figure 1. The synthetic approach used to construct the cross-link is shown in Scheme 1. Starting from 5′-*O*-dimethoxytrityl-3′-*O*-*tert*-butyldimethylsilyl-2′-deoxythymidine **1**, the N³ position of the heterocycle was alkylated using DBU and iodoalkyl phenoxyacetate to form adducts **3a**−**c** in a fashion similar to the synthesis of thymine or uracil nucleotide analogues that require protection of the N³ position.[28,29] Depending on the iodoalkane used, it is possible to synthesize adducts having linkers of various lengths. The phenoxyacetyl group was removed from **3a**−**c** using propylamine to the give the free alcohol, which was subsequently converted to iodide **4a**−**c** in good yield using triphenylphosphine, imidazole, and iodine.[24] The protected cross-link **5a**−**c** was then formed by deprotonating the N³−H of 5′-*O*-dimethoxytrityl-3′-*O*-phenoxyacetyl-deoxythymidine, **2**, with DBU, followed by the addition of iodo adduct **4a**−**c**. In the case of the four- and seven-carbon linker adducts the reaction proceeded

(28) Altmann, K. H.; Kesselring, R.; Francotte, E.; Rihs, G. *Tetrahedron Lett.* **1994**, *35*, 2331−2334.
(29) Krecmerova, M.; Hrebacebecky, J.; Holy, A. *Collect. Czech. Chem. Commun.* **1990**, *55*, 2521−2536.

Scheme 2. Construction of Cross-Linked Duplexes via Solid Phase Synthesis

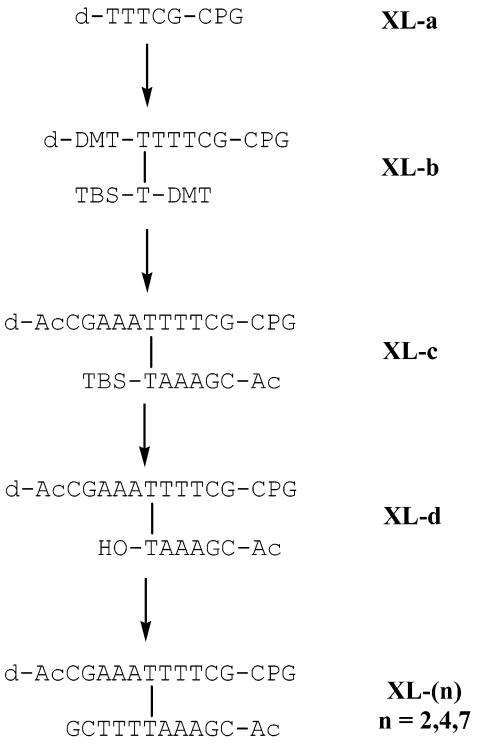

smoothly. However, initial attempts to synthesize the two-carbon linker adduct were not successful because of the conversion of iodo adduct **4a** to alcohol precursor **3a** when using two or more equivalents of DBU. This undesired side reaction was minimized by using 1 equiv of DBU when coupling **2** to **4a**. The 3′-*O*-phenoxyacetyl group of dimer **5a**−**c** was removed with propylamine to afford **6a**−**c**, which was then phosphitylated to give the protected cross-link phosphoramidites **7a**−**c** for solid-phase synthesis.

The solid-phase synthetic strategy used to prepare the cross-linked duplexes, which is similar to that used previously to prepare N^4C-alkyl-N^4C cross-linked duplexes,[18−21] is shown in Scheme 2. Syntheses were carried out on a 2 μmol scale. The first arm of the duplex, **XL-a**, was synthesized on a controlled pore glass support. The N^3T-alkyl-N^3T cross-link phosphoramidite **7a**−**c** was used to introduce the cross-link at the 5′ end of the oligomer to give **XL-b**. The dimethoxytrityl groups were removed by brief treatment with 2% dichloroacetic acid in methylene chloride. The second and third arms of the duplex were synthesized simultaneously by repetitive coupling with protected nucleoside-3′-phosphoramidites to give, after detritylation and acetylation, the branched Y-intermediate, **XL-c**. The *tert*-butyldimethylsilyl (TBDMS) group was then removed from **XL-c** by treating the support with anhydrous tetra-*n*-butylammonium fluoride (TBAF) in tetrahydrofuran. Because fluoride-mediated desilylation can result in cleavage of adjacent β-cyanoethylphosphotriester linkages,[30] **XL-c** was first treated with anhydrous triethylamine to convert the triester groups to phosphodiester linkages. A similar strategy was used previously in the synthesis of branched oligoribonucleotides and in the syntheses of DNA duplexes containing N^4C-alkyl-N^4C interstrand cross-links.[18−21,30] In addition, treatment of the support with TBAF was limited to a reaction time of 20 min as extended treatment results in significant cleavage of the oligonucleotide from the solid support, a result shown previously by Damha et al. in model studies using DMT-dT-(LCAA-CPG).[30] To determine the extent of removal of the silyl group, a small amount (approximately 1 mg) of CPG was treated with a mixture of concentrated ammonium hydroxide/ethanol (3:1) at 55 °C for 4 h. These conditions deprotect RNA without loss of the silyl group. The hydrolyzate was analyzed by C-18 reversed-phase HPLC. The desilyated oligomers, **XL-d**, have a shorter retention time on the reversed-phase column and are easily distinguished from the slower moving silyated oligomers, **XL-c**. Removal of the TBDMS group by treatment of the Y-intermediate with TBAF resulted in variable yields of desilylation with the different oligomers. For example, in the case of the four-carbon linker, the removal of the TBDMS group was quantitative; however, in the case of the two- and seven-carbon linkers, the TBDMS group was removed 50 and 61%, respectively. Variable amounts of desilation have also been observed previously in the synthesis of N^4C-alkyl-N^4C cross-linked duplexes.[18−21]

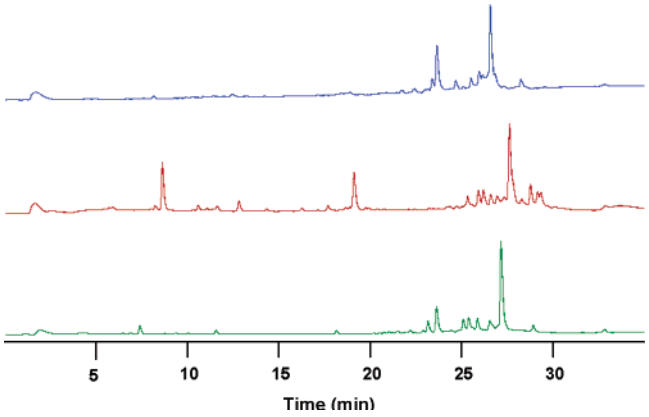

Figure 2. Strong anion exchange HPLC profiles of crude **XL-2** (blue), **XL-4** (red), and **XL-7** (green). The column, which was monitored at 260 nm, was eluted with a gradient of 0−0.5 M sodium chloride in 100 mM Tris-HCl, pH 7.8, 10% acetonitrile, at a flow rate of 1.0 mL/min.

The full-length cross-linked duplexes, **XL-2**, **4**, and **7**, were prepared by repetitive coupling of the 3′-end of the Y-intermediate **XL-d** with protected nucleoside 5′-phosphoramidites. To maximize the coupling yields, the phosphoramidites were used at a concentration of 0.3 M instead of the usual 0.15 M concentration used for nucleoside 3′-phosphoramidites. In addition, it was found necessary to increase the total detritylation time to 130 s to effect complete removal of the 3′-*O*-dimethoxytrityl groups.

The cross-linked oligomers were deprotected by treating the support with a mixture of concentrated ammonium hydroxide/ethanol (3:1) at 55 °C for 4 h. The duplexes were purified by strong anion exchange HPLC using a sodium chloride gradient in buffer that contained 100 mM Tris-HCl and 10% acetonitrile as shown in Figure 2. The major side product in these syntheses was the deprotected form of **XL-c**, which resulted from incomplete desilylation of the TBS-protected Y-intermediate. The duplexes, whose retention times are shown in Table 1, eluted as single peaks and were obtained in approximately 8−16% isolated and 5−6% overall yield. Despite the low overall yield, this procedure provides sufficient quantities of cross-linked

(30) Braich, R. S.; Damha, M. J. *Bioconjugate Chem.* **1997**, *8*, 370−377.

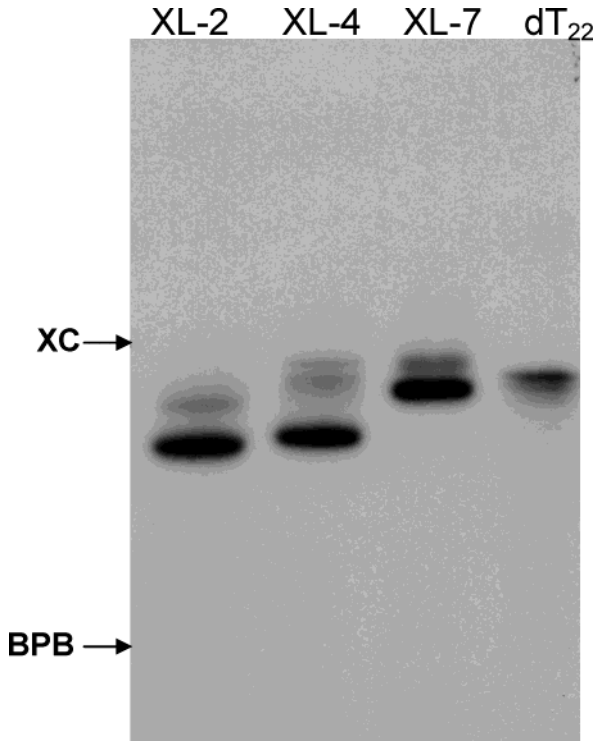

Figure 3. Polyacrylamide gel electrophoresis of cross-linked duplexes. Cross-linked duplexes **XL-2** (lane 1), **XL-4** (lane 2), **XL-7** (lane 3), and a control oligomer, dT_{22} (lane 4) were each 5′ end-labeled with γ[^{32}P]-ATP and subjected to electrophoresis on a 20% polyacrylamide gel run under denaturing conditions. XC and BPB are xylene cyanol and bromophenol blue dyes, respectively.

oligomers for biological and physical studies, including structural studies by high-resolution NMR spectroscopy.

Samples of each duplex were digested with a combination of snake venom phosphodiesterase and calf intestinal phosphatase, and the digests were analyzed by C-18 reversed-phase HPLC. As shown in Table 1, each duplex was hydrolyzed to its component nucleosides and the N^3T-alkyl-N^3T cross-link in ratios consistent with the structure of the particular duplex. In addition to this characterization, each duplex was analyzed by MALDI TOF mass spectrometry. As shown in Table 1, the resulting mass-to-charge ratios were consistent with the structure of the duplex. Analysis of the final products via electrophoresis on denaturing polyacrylamide gels, as shown in Figure 3, reveal that the cross-linked duplexes are of sufficient purity for structural and biological investigations.

Physical Studies. To evaluate the effect of the N^3-alkyl-N^3 cross-link on B-form DNA, molecular models of a T−T mismatch as well as those of the cross-linked duplexes containing the two-, four-, and seven-carbon linkers were generated using the program Hyperchem. These models were geometry-optimized using the Amber force field, with the final models shown in Figure 4. In all cases, the models predict that the cross-links should have little effect on the global structure of the duplexes. Thus, the overall geometry of the cross-linked duplexes appears to be that of B-form DNA. The base pairs flanking the cross-link maintain Watson−Crick hydrogen bonding, although in the case of the four- and seven-carbon cross-links there appears to be some buckling of the neighboring base pairs (Figure 4, models D and E). The N^3−N^3 distance of the T−T mismatch was found to be 3.8 Å. As expected, this distance increases as the length of the linker increases from two (3.6 Å) to four (6.1 Å) to seven (8.4 Å) methylene groups.

The prediction that the cross-links do not greatly affect the structure of B-form DNA was confirmed by CD spectra. The CD spectra of cross-linked duplexes **XL-2**, **XL-4**, and **XL-7** and the non-cross-linked control were recorded at 5 °C (Figure 5). Under these conditions, both the cross-linked and non-cross-linked oligomers should be in their base-paired, duplex form. In all cases, the CD spectra of the duplexes exhibit signatures characteristic of B-form DNA. In the case of **XL-4** and **XL-7**, the peak maxima are slightly blue-shifted relative to the non-cross-linked duplex and **XL-2**.

Ultraviolet thermal denaturation experiments were carried out to assess the effects of the various cross-links on duplex stability. Thermal denaturation curves for cross-linked duplexes **XL-2**, **XL-4**, **XL-7**, along with a non-cross-linked control duplex, which contains an A−T base pair in place of the T−T cross-link, are shown in Figure 6. The denaturation temperature, which is defined as the midpoint of the thermal denaturation curve, of each duplex is listed in Table 2. Each cross-linked oligomer displayed a sigmoidal denaturation profile. Although the overall hyperchromicities of the transition curves of the cross-linked duplexes and the non-cross-linked control are approximately the same, there are significant differences in the breadths of the denaturation curves. The breadth of the denaturation curve of **XL-2**, with a denaturation temperature of approximately 77 °C, is similar to that of the control duplex, suggesting that these duplexes denature in a highly cooperative manner. The much broader transitions seen for **XL-4** and **XL-7** suggest that these duplexes denature in a less cooperative manner than does **XL-2**.

As was seen previously with N^4C-alkyl-N^4C cross-linked duplexes,[18,20,21] the denaturation temperatures of the N^3T-alkyl-N^3T cross-linked duplexes are 16−37 °C higher than the melting temperature of the non-cross-linked control. This increased thermal stability is most likely a consequence of covalently linking the two strands of the duplex. Thus, denaturation/renaturation of the cross-linked duplex is a unimolecular process, which is independent of the strand concentration, whereas denaturation/renaturation of the non-cross-linked control is a unimolecular process for denaturation and bimolecular for renaturation.

The denaturation temperature of the cross-linked duplex is dependent upon the length of the N^3T-alkyl-N^3T cross-link. As seen in Table 2, the order of stability is **XL-2** > **XL-4** > **XL-7**. The denaturation temperatures of **XL-2** and **XL-4** differ by only 6 °C, whereas that of **XL-7** is 21 °C less than that of **XL-2**. A similar effect was seen for duplexes that contained a directly opposed N^4C-alkyl-N^4C-type interstrand cross-link.[18] Here the duplex with a two-carbon linker has the highest thermal denaturation temperature (25 °C higher than the control),[18] whereas duplexes with a three- or four-carbon linker have increased denaturation temperatures of 20 and 17 °C, respectively (unpublished results). For both two- and four-carbon linkers, the denaturation temperatures of the directly opposed N^3T-alkyl-N^3T cross-link is greater than those of the N^4C-alkyl-N^4C type interstrand cross-link.

The relative thermal stabilities of the duplexes are reflected in their electrophoretic mobilities on a denaturing polyacrylamide gel, as shown in Figure 3. Cross-linked duplexes

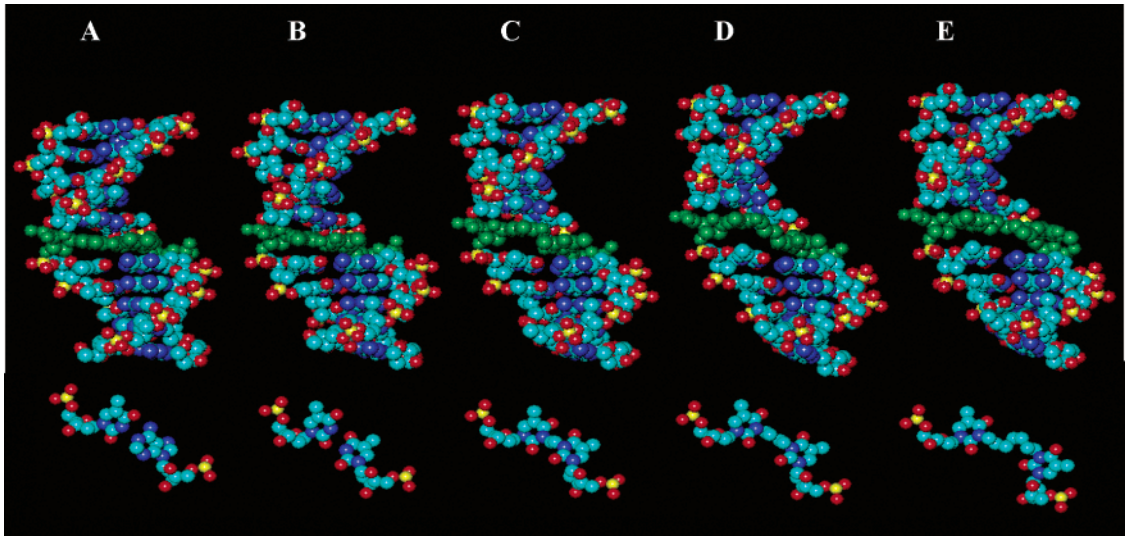

Figure 4. Molecular models of a (A) complementary duplex, d(CGAAATTTTCG)/d(GCTTTAAAAGC), (B) self-complementary duplex d(CGAAATTTTCG)$_2$ that contains a mismatched T−T, and self-complementary duplexes d(CGAAAT*TTTCG)$_2$ where T* is N3T-alkyl-N3T (shown in green) with alkyl linkers that are (C) two, (D) four, and (E) seven carbon atoms long. The models were built using Hyper Chem molecular modeling software and energy minimized using the Amber force-field.

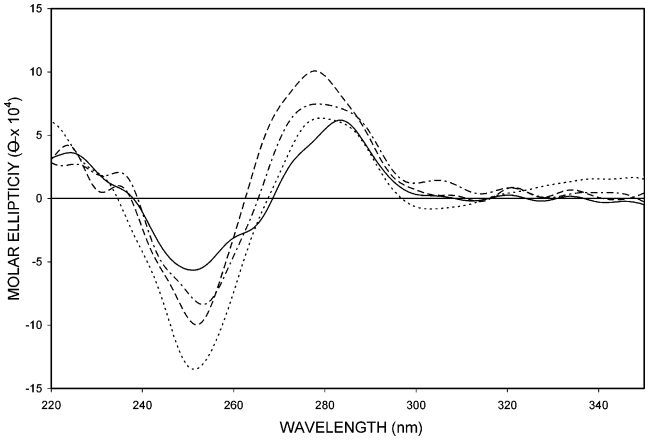

Figure 5. Circular dichroism spectra of cross-linked duplex **XL-2** (···), **XL-4** (− − −), **XL-7** (−·−), and non-cross-linked control (—). Solutions containing 1 μM duplex in 90 mM sodium chloride, 10 mM sodium phosphate, and 1 mM ethylenediaminetetraacetate buffer, pH 7.0, were heated at 0.5 °C/min. Spectra were recorded at 5 °C.

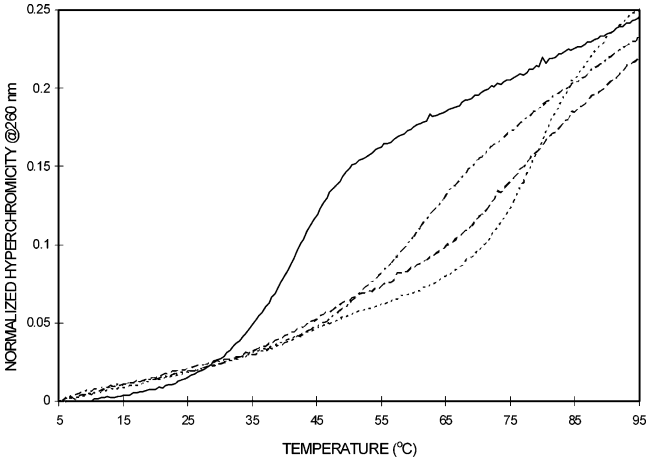

Figure 6. Absorbance (A_{260}) versus temperature profiles of cross-linked duplex **XL-2** (···), **XL-4** (− − −), **XL-7** (−·−), and non-cross-linked control (—). Solutions containing 2 μM duplex in 90 mM sodium chloride, 10 mM sodium phosphate, and 1 mM ethylenediaminetetraacetate buffer, pH 7.0, were heated at 0.5 °C/min.

XL-2 and **XL-4** each have a higher electrophoretic mobility than **XL-7**, whose mobility is similar to that of dT_{22}. It is unlikely that the difference in mobility between **XL-2** or **XL-4** and **XL-7** is due solely to the increased molecular weight of the cross-link. Rather, it appears that **XL-7**, which consists of 22 nucleotides, is denatured under the conditions of the experiment, whereas **XL-2** and **XL-4**, which have higher thermal stabilities, migrate as base-paired duplexes, even in the presence of 7 M urea. Similar behavior was seen when N^{4}C-alkyl-N^{4}C, −CNG−-type interstrand cross-linked duplexes were electrophoresed under denaturing conditions.[21] The thermally more stable four- and seven-carbon linked duplexes migrated with a higher mobility than the less stable two-carbon linked duplex.

Previous modeling and NMR studies of a C−C ethyl cross-linked duplex revealed that the ethyl linker protrudes into the major groove of the duplex.[19,31] This lesion induces an overall axis bend toward the major groove, narrowing of the major and minor grooves around the cross-link, and buckling of base pairs around the cross-linked site. In the case of the T−T ethyl cross-link, the lesion lies in neither the major nor minor groove but rather appears to pass through the helical axis. Models suggest that the length of the two-carbon cross-link is sufficient to span the distance between the N^3 atoms of the T−T mismatch without perturbing the helix structure and surrounding base pairs. Consequently, the two-carbon linked duplex has a high thermal stability relative to the non-cross-linked control. The longer

Table 2. Thermal Denaturation of Cross-Linked Duplexes and Their Non-Cross-Linked Controls

duplex	T_m (°C)[a]
XL-2	77
XL-4	71
XL-7	56
control	40

[a] Experiments were carried out in buffer containing 90 mM sodium chloride, 10 mM sodium phosphate, and 1 mM ethylenediaminetetraacetate buffer (pH 7.0). The concentration of each strand was 2 μM.

(31) da Silva, M. W.; Noronha, A. M.; Noll, D. M.; Miller, P. S.; Colvin, O. M.; Gamcsik, M. P. *Biochemistry* **2002**, *41*, 15181−15188.

linkers, particularly the seven-carbon linker, however, tend to push the thymines apart, creating a local distortion at the site of the cross-link and affecting base pairs on either side of the cross-link. The relatively lower thermal stability of the seven-carbon cross-linked duplex reflects this perturbation. Further insights into the structures of these duplexes await high resolution NMR analyses, which are currently in progress.

The T−T cross-link mimics to some extent C−C and G−C-type cross-links in that linkage occurs at the N^3 position of the pyrimidine base. Because alkylation at this site can potentially interfere with base pairing, this type of lesion would be expected to present a serious obstacle to faithful repair of the lesion. We are currently testing this hypothesis by studying repair of T−T cross-linked DNA in cell extracts and whole cells.

Acknowledgment. This research was supported by a grant from the National Cancer Institute (CA082785). A.M.N. and C.J.W. were each supported in part by postdoctoral fellowships from the Natural Sciences and Engineering Research Council of Canada (NSERC).

JA0498540